



Analysis of Energy Accumulation and Dispersion Evolution of a Thick Hard Roof and Dynamic Load Response of the Hydraulic Support in a Large Space Stope

Qingwei Bu^{1,2†}, Min Tu^{1*†}, Xiangyang Zhang¹, Ming Zhang³ and Qingchong Zhao¹

¹Key Laboratory of Safety and High-Efficiency Coal Mining of Ministry of Education, Anhui University of Science and Technology, Huainan, China, ²School of Mining and Coal, Inner Mongolia University of Science and Technology, Baotou, China, ³State Key Laboratory of Mining Response and Disaster Prevention and Control in Deep Coal Mines, Anhui University of Science and Technology, Huainan, China

OPEN ACCESS

Edited by:

Kun Du,
Central South University, China

Reviewed by:

Liang Chen,
Guangdong University of Technology,
China

Liang Chen,
China University of Mining and
Technology, China

*Correspondence:

Min Tu
mtu@aust.edu.cn

†ORCID:

Qingwei Bu
orcid.org/0000-0002-4628-856X

Min Tu
orcid.org/0000-0002-1215-9639

Specialty section:

This article was submitted to
Geohazards and Georisks,
a section of the journal
Frontiers in Earth Science

Received: 26 February 2022

Accepted: 24 March 2022

Published: 26 May 2022

Citation:

Bu Q, Tu M, Zhang X, Zhang M and
Zhao Q (2022) Analysis of Energy
Accumulation and Dispersion
Evolution of a Thick Hard Roof and
Dynamic Load Response of the
Hydraulic Support in a Large
Space Stope.
Front. Earth Sci. 10:884361.
doi: 10.3389/feart.2022.884361

Aiming at the mining disaster of a thick hard roof, based on the analysis of the mining instability influence of the thick hard roof, this study constructs the mining bearing mechanical model of the thick hard roof by using mechanical theory and obtains the mechanical distribution equation of mining bearing and energy accumulation, the mining instability energy release equation, and the dynamic load response equation of a hydraulic support in the working face, as well as the dynamic load response characteristics of the hydraulic support in the working face, putting forward the technical countermeasures for the strong dynamic pressure control of the thick hard roof in the working face. This research shows that 1) the larger the overburden load and suspension span of the thick hard roof, the more serious the mining bearing state and energy accumulation evolution; the greater the rock thickness and elastic modulus of the thick hard roof, the greater the flexural stiffness of the roof, resulting in the increase of the roof mining limit breaking span, which indirectly aggravates the mining bearing state and self-energy accumulation evolution; 2) the dynamic support resistance of the hydraulic support is composed of the dynamic support resistance caused by the release of elastic energy accumulated by mining of the thick hard roof, the work done by the overlying load, and the static support resistance caused by the direct roof gravity; 3) the dynamic support resistance caused by the work of the overlying load accounts for the highest proportion, followed by the dynamic support resistance caused by the release of mining elastic energy by the thick hard roof; the cause of mining instability and the strong dynamic pressure of the thick hard roof lie in the large span of the mining suspended roof, and the large-scale mining suspension structure of the thick hard roof leads to a high overlying load and large accumulated energy; and 4) the mining instability of the thick hard roof leads to a strong dynamic load response of the hydraulic support; adopting pre-splitting and roof cutting technology to reduce the breaking span of the thick hard roof and reducing the impact dynamic load caused by mining instability of the thick hard roof can effectively eliminate the potential safety hazard of overlimit bearing of the hydraulic support.

Keywords: large space stope, thick hard roof, mining instability, energy accumulation and dispersion, hydraulic support, dynamic pressure disaster

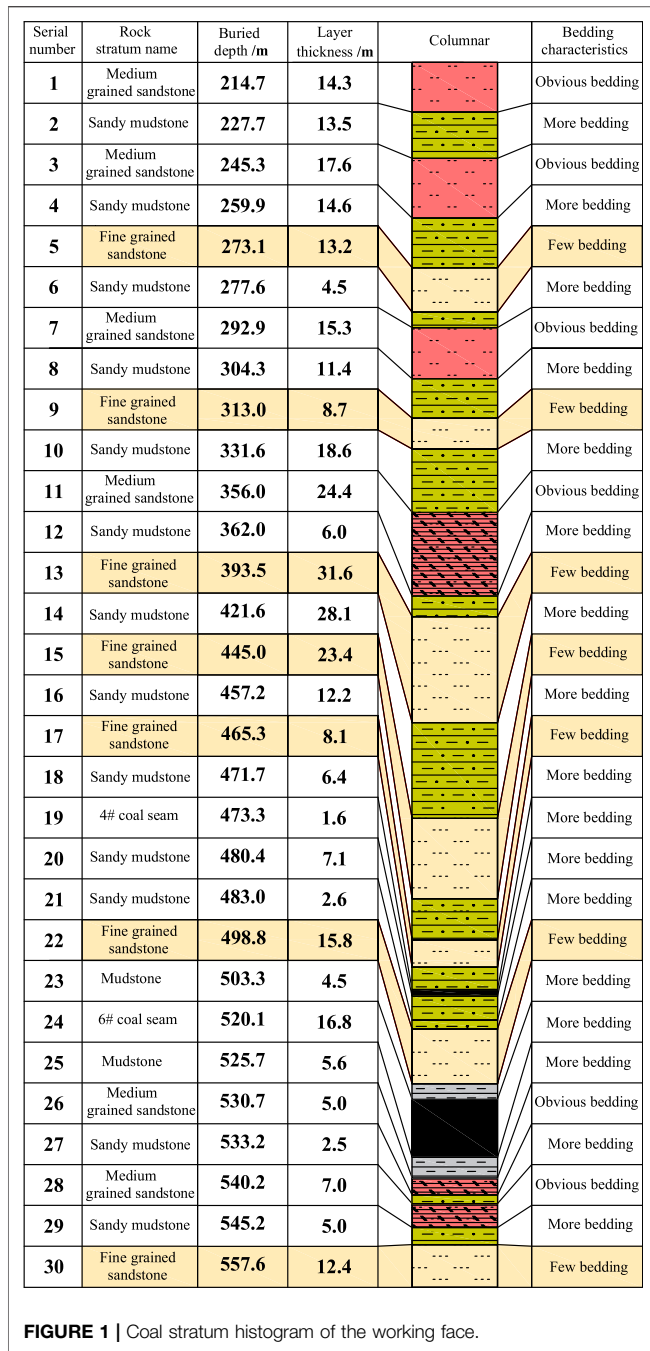
INTRODUCTION

The geological conditions of the thick hard roof in coal mines are becoming more and more common, the dynamic pressure of mining instability of the thick hard roof is particularly strong, and the hidden danger of the strong dynamic pressure disaster in the working face is serious. In many coal mines in Inner Mongolia, the deep coal measure strata generally contain thick and hard strata dominated by fine sandstone and conglomerate, which have a large thickness, high strength, and no obvious bedding fissures. In the deep part of coal measure strata, the thick and hard rock stratum forms a plate beam bearing structure with a long-span suspension and is difficult to collapse; once the plate beam bearing structure reaches the bearing limit, it will cause a strong dynamic pressure impact on the stope space, which is a serious threat to the safe and efficient mining of coal mines.

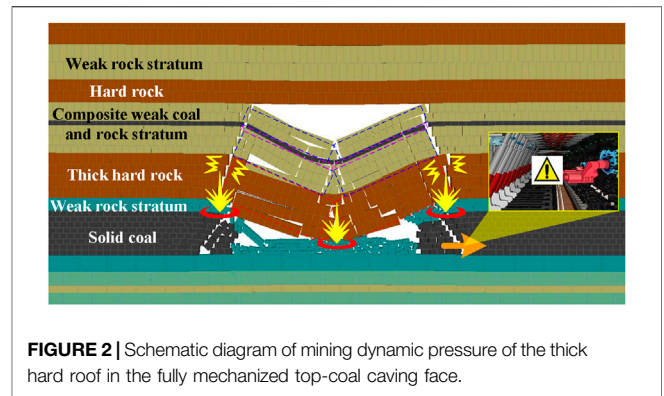
In order to ensure the safe and efficient mining of coal mines, many scholars pay special attention to the problem of mining pressure disasters under thick hard roof conditions. In terms of mining disaster analysis under thick hard roof conditions and by the investigation and measurement of the ground pressure in the working face with a thick hard roof, it is concluded that a phenomenon of the strong ground pressure exists in the working face with a thick hard roof, a large number of elastic properties are accumulated in the thick and hard rock itself with the coal and rock volume under it, and the mining instability of the thick hard roof has a hidden danger of inducing rock burst and air blast disaster in the working face (Christopher and Michael, 2016; Iannacchione and Tadolini, 2016; Tan et al., 2019). Through the analysis of the stope ground pressure behavior under thick hard roof conditions, it is revealed that the instability of the thick and hard rock structure in a large space stope leads to the strong ground pressure behavior of the working face, and the classification evaluation model of the ground pressure strength is established to guide the prediction and pre-control of the ground pressure disaster in hard roof coal seam mining (Xia et al., 2017; Dou et al., 2020; Gao et al., 2020). Some scholars have carried out microseismic monitoring of the overlying rock of the stope under thick hard roof conditions, analyzed the vibration response of the mining fracture of the overlying rock of the stope, and revealed the elastic release and propagation characteristics of its accumulation caused by the mining fracture of the thick and hard roof (Lu et al., 2015; Zhang et al., 2017). Facing the disaster problem of mining instability of the thick hard roof, some scholars have carried out technical countermeasures such as solid filling and blasting roof cutting and achieved good engineering results, avoiding the disastrous disturbance of the thick hard roof structure instability on the stope and roadway (He et al., 2012; Zhang et al., 2016). The stability analysis of the working face hydraulic support under the condition of the thick hard roof was carried out. Based on the key layer theory and composite beam mechanical model, a calculation method of the static resistance of the support in a fully mechanized top-coal caving face is proposed (Zhao et al., 2017). By analyzing the influence of mining instability of the thick hard roof on the stability of the hydraulic support in the working face, it is concluded that the support stiffness is positively

correlated with the support resistance. Manual roof cutting is adopted to reduce the fracture length of the roof and cooperate with it to achieve the purpose of roof control (Yu et al., 2013; Song et al., 2020). By analyzing the pressure behavior characteristics of the hydraulic support of the working face when the thick hard roof is broken, this study reveals the impact dynamic pressure behavior of the mining failure of the basic roof of the thick and hard rock stratum on the lower direct roof and support and proves that the dynamic load of the working face is much greater than the pressure effect of the hydraulic support caused by the static load (Yang et al., 2017). In the analysis of the mining instability mechanism of the thick hard roof, some scholars have successively adopted the elastic foundation orthogonal beam model, fixed beam mechanical model, and composite beam structure model considering a horizontal force to study the mechanical mechanisms of mining instability of the hard roof in a stope, such as bending deformation, instability span, and stress transfer of the hard roof (Jiang et al., 2016; Zuo et al., 2017; Zhang et al., 2020). According to the bearing mechanical characteristics of the thick hard roof, scholars use the elastic foundation beam model to analyze the distribution characteristics of deflection, bending moment, and energy accumulation of the hard roof (Li et al., 2007; Gu et al., 2018). Some scholars also use the medium-thick plate theory and finite element method to analyze the mining stress and fracture evolution of the hard and thick roof in the stope space (Xie et al., 2016; Yang et al., 2020). At present, many research studies mainly analyze the hard roof slab in the stope space as a thin beam or a thin plate structure but it is not applicable to the hard rock stratum with large thickness. Although some scholars use the elastic mechanic's solution method to analyze the fixed supported thick beam or fixed supported medium and thick plate structure, the fixed support boundary is different from the clamped support boundary constraint of the actual situation, and the analyzed mining energy accumulation and fracture instability position of the thick hard roof are deviated from the actual situation; the spatial state equation analysis method and finite difference analysis method of the plate structure are complex, difficult to study in depth, and have a little advantage in popularizing and using engineering technology. Therefore, the mechanical model suitable for the analysis of the mining bearing capacity of the thick hard roof still needs to be further studied.

To sum up, many scholars have made a lot of research achievements in the study of mining disasters under thick hard roof conditions. However, the mining disasters under the conditions of a thick hard roof, such as the energy accumulation and dispersion evolution before and after the mining fracture of a thick hard roof, the mining instability of the thick hard roof, the difference between dynamic and static pressure, and the strong dynamic load response of the hydraulic support in the working face, need to be further analyzed and studied. Therefore, combined with engineering examples, based on the analysis of the mining influence characteristics of thick hard roof conditions, this study constructs the mechanical model of mining bearing structure of thick hard roof by using the mechanical analysis method of single generalized displacement thick beam and the mechanical theory of semi-infinite elastic foundation beam and



analyzes the mechanical law of mining bearing and energy accumulation of thick hard roof. According to the energy principle, the mechanical equations of energy accumulation and dispersion of thick hard roof and dynamic load response of hydraulic support in a large space stope are deduced, the dynamic load response of hydraulic support for mining instability of thick hard roof in working face is analyzed, and then the technical countermeasures for the strong ground pressure control of thick hard roof are put forward. This study provides a reference for the strong dynamic pressure behavior of similar thick hard



roofs and the dynamic pressure bearing analysis of hydraulic support.

ANALYSIS OF MINING INSTABILITY CHARACTERISTICS OF THE THICK HARD ROOF IN THE WORKING FACE

Engineering General Situation of the Working Face With the Thick Hard Roof

In the 61304 fully mechanized top-coal caving face in the Tangjiahui coal mine, the 6# coal seam is the main coal seam; the minable thickness of this coal seam is 16.8 m, the average dip angle of the coal seam is 2°, the strike length of the working face is 2,141 m, the dip width is 240 m, the fully mechanized mining height is 4.5 m, and the caving height is 12.3 m. The occurrence structure of the coal measure strata is shown in **Figure 1**; the direct roof of the main mining coal seam is 4.5 m thick argillaceous rock, and the overlying basic roof is 15.8 m thick fine sandstone, which is mainly composed of a 4# coal seam, sandy mudstone, medium-grained sandstone, and fine sandstone; among the aforementioned rock layers, mudstone, sandy mudstone, and medium-grained sandstone layers show obvious bedding fracture development, argillaceous weak cementation, locally mixed with loose conglomerate, and the overall strength is low but the fine sandstone layer is thick, hard and has high mechanical strength. There is a hidden danger of strong dynamic pressure disaster caused by mining instability of the long-span suspended roof.

Influence Characteristics of Mining Instability of the Working Face Under the Thick Hard Roof

By investigating the ground pressure behavior of the mined working face in the Tangjiahui coal mine, it is found that during the mining process, the direct roof of mudstone collapses with the top-coal caving mining, as shown in **Figure 2**, the thick hard roof of fine sandstone overlying it presents a plate beam suspension-bearing structure with long-span suspension and is difficult to collapse. The breaking and instability of the bearing structure of the thick hard roof cause the strong dynamic ground pressure at the moment, which poses a

serious threat to the safety of mining, support equipment, and operators of the working face.

In view of the mining influence of thick hard roof conditions, combined with relevant ground pressure theory and engineering experience, the mining instability influence of the thick hard roof in the working face is analyzed from four aspects: bearing state, spatial structure, instability energy release, and dynamic and static pressure difference:

- (1) From the analysis of the stope space, after mining in the longwall coal face of fully mechanized top-coal caving, spatial mining suspended roof structure with a suspended span of 60–80 m and transverse width of 240 m is formed. Once this large area of the suspended roof is unstable, it will show an air impact on the mining space.
- (2) From the aspect of roof bearing, the thick and hard roof has a large thickness and relatively high strength, so it has a strong mechanical bearing capacity; in the process of on-site face mining, the thick and hard roof presents a safety risk situation of difficult collapse and large hanging span.
- (3) From the analysis of the difference between the dynamic and static pressure, compared with the mining instability of the general thin and weak strata, the mining instability pressure of the thick and hard roof is strong, especially the impact dynamic load of the thick and hard roof at the low position of the stope space is particularly obvious to the dynamic pressure of the working face below.
- (4) From the analysis of the pressure behavior of the working face, the instability of the long-span suspension structure will cause mining instability and dynamic load behavior of the broken rock block below and the hydraulic support of the working face, resulting in a large safety deviation between the resistance of the hydraulic support calculated according to the static load and the actual situation.

According to the above safety impact analysis, the problem of strong dynamic pressure disaster of the thick and hard roof urgently needs to be studied and solved, including how to pre-judge the mining instability impact of the thick and hard roof, how to evaluate the dynamic pressure-bearing stability of the hydraulic support in the working face, and what is the key to control the display of the strong dynamic pressure of the thick and hard roof. Therefore, the analysis of energy accumulation and dispersion evolution of the thick hard roof and dynamic load response of the hydraulic support in a large space stope is of great value to solve the problem of strong dynamic pressure disaster of this kind of a thick and hard roof.

MECHANICAL MODEL ANALYSIS OF MINING BEARING CAPACITY AND ENERGY ACCUMULATION OF THE THICK HARD ROOF

Based on the analysis of the influence characteristics of mining instability of the thick hard roof in the working face, this study

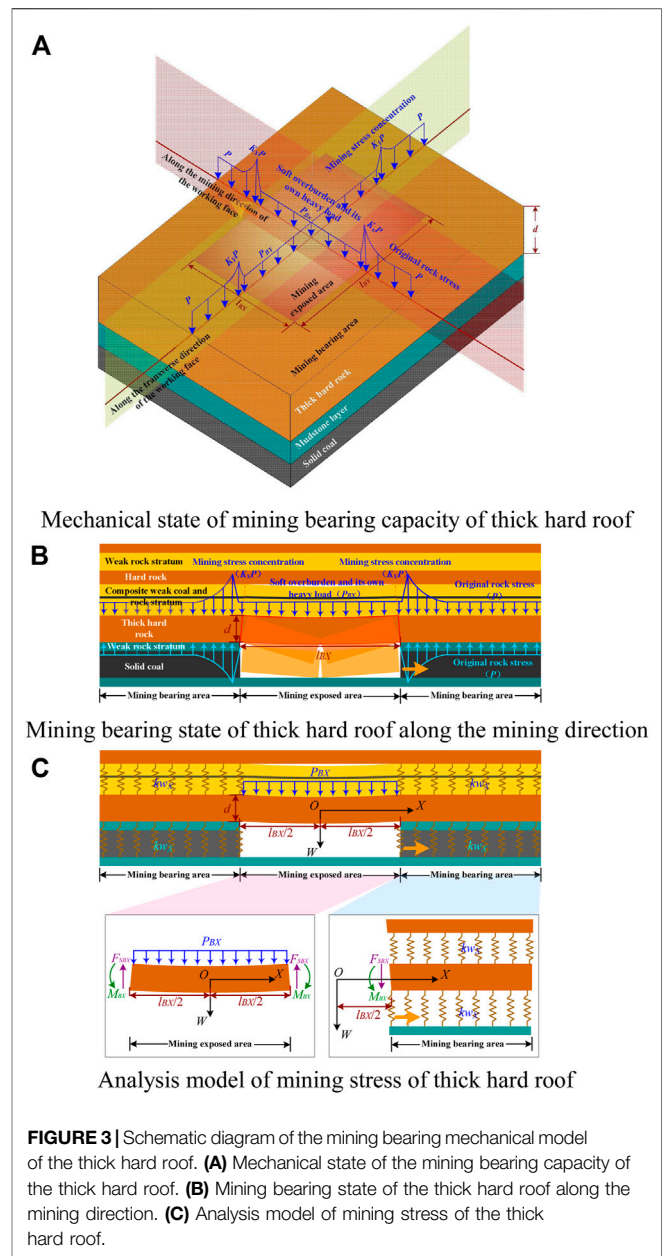


FIGURE 3 | Schematic diagram of the mining bearing mechanical model of the thick hard roof. **(A)** Mechanical state of the mining bearing capacity of the thick hard roof. **(B)** Mining bearing state of the thick hard roof along the mining direction. **(C)** Analysis model of mining stress of the thick hard roof.

considers the thick and hard rock roof as the research object, carries out the mechanical model analysis of mining bearing and energy accumulation of the thick hard roof, and reveals the characteristic law of mining bearing and energy accumulation of the thick hard roof, which provides a research basis for the analysis of mining instability and dynamic pressure influence of the thick hard roof in a large space stope.

Construction of the Mining Bearing Mechanical Model of the Thick Hard Roof

In order to reasonably analyze the mechanical evolution mechanism of mining bearing and energy accumulation of the thick hard roof, based on the MARCUS simplified algorithm, this

study constructs the mechanical model of mining bearing of the thick hard roof by using the mechanical analysis method of a single generalized displacement thick beam and the mechanical theory of the semi-infinite elastic foundation beam, as shown in **Figure 3**.

In order to facilitate the solution and analysis of the mechanical model, the following basic assumptions are made for the mining bearing mechanical model of the thick hard roof:

- (1) According to the analysis of the law of stope roof activity, for the longwall mining of underground coal mines, the span width ratio of the stope space roof is small and the flat strain beam structure can be used for mechanical analysis.
- (2) Consider the middle of the exposed area before the mining fracture of the thick hard roof as the origin of the mechanical coordinate system; then, the mining direction along the working face is the X-coordinate axis and the vertical direction is the W-coordinate axis, as shown in **Figure 3B**.
- (3) Set the overhang span of the thick hard roof as l_{BX} in the established mechanical coordinate system; then, the location of the mining overhang area in the stope space is $(-l_{BX}/2, l_{BX}/2)$ and the mining bearing area is $(l_{BX}/2, +\infty)$.
- (4) In the mining exposed area $(-l_{BX}/2, l_{BX}/2)$, the stress state of the thick hard roof can be regarded as a beam structure under a uniform load, and the overlying load p_{BX} of the roof in the exposed area is composed of its own rock load and the overlying soft coal and rock load.
- (5) Considering the large thickness span ratio of the thick hard top slab beam structure in the mining exposed area, the mechanical analysis of the thick beam structure with a single generalized displacement is carried out by using the mechanical model of the thick beam structure.
- (6) In the mining bearing area $(l_{BX}/2, +\infty)$, the thick hard roof is constrained by the upper and lower strata and presents the mechanical characteristics of the sandwich bearing, as shown in **Figure 3B**; according to the analysis of the activity law of the stope roof, the upper and lower strata of the stope thick hard roof can be regarded as the elastic foundation structure and analyzed with the mechanical model of the semi-infinite elastic foundation beam structure.
- (7) In the deep part of the mining bearing area, the mining stress load on the upper boundary and the foundation reaction load on the lower boundary interact with each other, so it can be regarded as the mutual balance and offset of forces in the mechanical analysis, thereby simplifying the analysis of the mining bearing mechanical model of the thick hard roof, as shown in **Figure 3C**.

Analysis of the Mining Bearing Mechanical Model of the Thick Hard Roof

According to the mechanical model shown in **Figure 3C**, the unit-wide strip of the thick hard top slab along the mining direction (x -axis) of the working face is considered as the research object, and the basic mechanical equation of the thick beam structure using a single generalized displacement method (Ke, 2000) is as follows:

$$\begin{cases} \theta_{BX} = \frac{dw_{BX}}{dx} + \frac{EI}{T} \frac{d^3w_{BX}}{dx^3}, \\ M_{BX} = -EI \left(\frac{d^2w_{BX}}{dx^2} + \frac{EI}{T} \frac{d^4w_{BX}}{dx^4} \right), \\ F_{SBX} = -EI \frac{d^3w_{BX}}{dx^3}, \\ -EI \frac{d^4w_{BX}}{dx^4} = -p_{BX}, \end{cases} \quad (1)$$

where w_{BX} is the deflection of the thick hard roof in the mining exposed area along the mining direction; p_{BX} is the overlying load composed of its own gravity load and the transmission load of the overlying weak rock stratum along the mining direction; θ_{BX} is the bending angle of the thick hard roof in the mining exposed area along the mining direction; M_{BX} is the bending moment of the thick hard roof in the mining exposed area along the mining direction; F_{SBX} is the shear force of the thick hard roof in the mining exposed area along the mining direction; E is the elastic modulus of the rock stratum—in plane strain problem, $E = E/(1-\nu^2)$; $I (=bd^3/12)$ is the polar moment of inertia; b is the structural width of the thick hard roof strip, taking unit width 1; d is the thickness of the thick hard roof; $T (=5Ebd/[12(1+\nu)])$ is the shear stiffness of the rectangular strip with the thick hard roof; and ν is Poisson's ratio—in a plane strain problem, $\nu = \nu/(1-\nu)$.

From the last equation of **Eq. 1**, the deflection equation of a single generalized displacement of the thick hard roof can be established, and the general solution is as follows:

$$w_{BX} = \frac{p_{BX}}{24EI}x^4 + \frac{B_{1X}}{6}x^3 + \frac{B_{2X}}{2}x^2 + B_{3X}x + B_{4X}, \quad (2)$$

where B_{1X} , B_{2X} , B_{3X} , and B_{4X} are undetermined coefficients.

Substituting **Eq. 2** into equations (1)–(3) of **Eq. 1**, and sorting out.

$$\begin{cases} \theta_{BX} = \frac{p_{BX}}{6EI}x^3 + \frac{B_{1X}}{2}x^2 + \left(B_{2X} + \frac{p_{BX}}{T} \right)x + B_{3X} + \frac{EIB_{1X}}{T}, \\ M_{BX} = -EI \left(\frac{p_{BX}}{2EI}x^2 + B_{1X}x + B_{2X} + \frac{p_{BX}}{T} \right), \\ F_{SBX} = -EI \left(\frac{p_{BX}}{EI}x + B_{1X} \right), \end{cases} \quad (3)$$

In the mining exposed area $(-l_{BX}/2, l_{BX}/2)$, the stress bending of the thick hard roof is axisymmetric along the centerline ($x = 0$), which shows that $\theta_{BX}|_{x=0} = 0$, $F_{SBX}|_{x=0} = 0$.

Solution: $B_{1X} = 0$; $B_{3X} = 0$

In **Eq. 3**, only B_{2X} and B_{4X} are unknown coefficients to be determined.

In the mining bearing area of overburden $(l_{BX}/2, +\infty)$, the mechanical equation of the elastic foundation strip structure is as follows:

$$EIw_{AX}^{(4)} = -kw_{AX}, \quad (4)$$

where w_{AX} is the curvature of the thick hard roof in the mining bearing area along the mining direction and k is the elastic foundation stiffness of the upper and lower boundary strata in the mining bearing area of the thick hard roof.

Let $\alpha_A = \sqrt[4]{k/4EI}$; **Eq. 4** is sorted as follows:

$$w_{AX}^{(4)} + 4\alpha_A^4 w_{AX} = 0, \tag{5}$$

In the mining bearing area, the general solution equation of deflection under the elastic foundation state of the thick hard roof is as follows:

$$w_{AX0} = A_{1X} [CC(x) - SC(x)] + A_{2X} [CS(x) - SS(x)], \tag{6}$$

where: $CC(x) = \cosh[\alpha_A(x - \frac{l_{BX}}{2})] \cos[\alpha_A(x - \frac{l_{BX}}{2})]$; $SC(x) = \sinh[\alpha_A(x - \frac{l_{BX}}{2})] \cos[\alpha_A(x - \frac{l_{BX}}{2})]$; $CS(x) = \cosh[\alpha_A(x - \frac{l_{BX}}{2})] \sin[\alpha_A(x - \frac{l_{BX}}{2})]$; and $SS(x) = \sinh[\alpha_A(x - \frac{l_{BX}}{2})] \sin[\alpha_A(x - \frac{l_{BX}}{2})]$.

In the mining bearing area, the mechanical analysis of the semi-infinite thick hard roof can still be analyzed according to the slender strip structure of elastic foundation as follows:

$$\begin{cases} \theta_{AX} = \frac{dw_{AX}}{dx}, \\ M_{AX} = -EI \frac{d^2 w_{AX}}{dx^2}, \\ F_{SAX} = -EI \frac{d^3 w_{AX}}{dx^3}, \end{cases} \tag{7}$$

where θ_{AX} is the curvature of the thick hard roof in the mining bearing area along the mining direction; M_{AX} is the bending moment of the thick hard roof in the mining bearing area along the mining direction; and F_{SAX} is the shear force of the thick hard roof in the mining bearing area along the mining direction.

The mechanical equation of the semi-infinite thick roof strip structure in the mining bearing area is as follows:

$$\begin{cases} \theta_{AX} = \{-\alpha_A(A_{1X} + A_{2X})[CS(x) - SS(x)] + \alpha_A(A_{1X} - A_{2X})[SC(x) - CC(x)]\}, \\ M_{AX} = -2\alpha_A^2 EI \{-A_{1X}[SS(x) - CS(x)] + A_{2X}[SC(x) - CC(x)]\}, \\ F_{SAX} = -2\alpha_A^3 EI \{-A_{1X}[CS(x) - SS(x)] - (A_{1X} + A_{2X})[SC(x) - CC(x)]\}, \end{cases} \tag{8}$$

Currently, A_{1X} and A_{2X} are undetermined coefficients.

At the end of the mining exposed area, the stress and deformation of the thick hard roof meet the static equivalent, that is, on both sides of the position ($x = l_{BX}/2$).

$$\begin{cases} w_{AX}|_{x=l_{BX}/2} = w_{BX}|_{x=l_{BX}/2}, \\ \theta_{AX}|_{x=l_{BX}/2} = \theta_{BX}|_{x=l_{BX}/2}, \\ M_{AX}|_{x=l_{BX}/2} = M_{BX}|_{x=l_{BX}/2}, \\ F_{SAX}|_{x=l_{BX}/2} = F_{SBX}|_{x=l_{BX}/2}, \end{cases} \tag{9}$$

Substituting Eqs 3 and 8 into Eq. 9, we obtain the following equations:

$$\begin{cases} A_{1X} = \frac{P_{BX}}{24EI} \left(\frac{l_{BX}}{2}\right)^4 + \frac{B_{2X}}{2} \left(\frac{l_{BX}}{2}\right)^2 + B_{4X} \\ -\alpha_B(A_{1X} - A_{2X}) = \frac{P_{BX}}{6EI} \left(\frac{l_{BX}}{2}\right)^3 + \left(B_{2X} + \frac{P_{BX}}{T}\right) \left(\frac{l_{BX}}{2}\right), \\ 2\alpha_B^2 EI A_{2X} = -\left[\frac{P_{BX}}{2} \left(\frac{l_{BX}}{2}\right)^2 + \left(B_{2X} + \frac{P_{BX}}{T}\right) EI\right] \\ -2\alpha_B^3 EI (A_{1X} + A_{2X}) = -P_{BX} \left(\frac{l_{BX}}{2}\right), \end{cases} \tag{10}$$

The coefficients are as follows:

$$\begin{cases} B_{2X} = \frac{P_{BX} l_{BX}}{8\alpha_A EI} \left(\frac{1}{-\frac{l_{BX}}{4\alpha_A} - \frac{1}{2\alpha_A^2}}\right) \left(\frac{1}{\alpha_A^2} + \frac{l_{BX}^2}{12} + \frac{l_{BX}}{2\alpha_A}\right) - \frac{P_{BX}}{T}, \\ B_{4X} = \frac{P_{BX} l_{BX}}{8EI} \left(\frac{1}{\alpha_A^3} - \frac{l_{BX}^2}{16\alpha_A} - \frac{l_{BX}^3}{48} - \frac{2EI}{\alpha_A T}\right) - B_{2X} \left(\frac{l_{BX}}{4\alpha_A} + \frac{l_{BX}^2}{8}\right), \\ A_{1X} = \frac{P_{BX} l_{BX}}{8EI} \left(\frac{1}{\alpha_A^3} - \frac{l_{BX}^2}{16\alpha_A}\right) - \frac{l_{BX}}{4\alpha_A} \left(B_{2X} + \frac{P_{BX}}{T}\right), \\ A_{2X} = \frac{P_{BX} l_{BX}}{8EI} \left(\frac{1}{\alpha_A^3} + \frac{l_{BX}^2}{16\alpha_A}\right) + \frac{l_{BX}}{4\alpha_A} \left(B_{2X} + \frac{P_{BX}}{T}\right), \end{cases} \tag{11}$$

The bending deformation equation of the thick hard roof in the stope space along the working face direction (X-axis) can be sorted out as follows:

$$w_{ABX} = \begin{cases} A_{1X} [CC(-x) - SC(-x)] + A_{2X} [CS(-x) - SS(-x)] \left(-\infty, -\frac{l_{BX}}{2}\right) \\ \frac{P_{BX}}{24EI} x^4 + \frac{B_{2X}}{2} x^2 + B_{4X} \left[-\frac{l_{BX}}{2}, \frac{l_{BX}}{2}\right] \\ A_{1X} [CC(x) - SC(x)] + A_{2X} [CS(x) - SS(x)] \left[\frac{l_{BX}}{2}, +\infty\right), \end{cases} \tag{12}$$

$$M_{ABX} = \begin{cases} -2\alpha_A^2 EI \{-A_{1X}[SS(-x) - CS(-x)] + A_{2X}[SC(-x) - CC(-x)]\} \left(-\infty, -\frac{l_{BX}}{2}\right) \\ -\left(\frac{P_{BX}}{2} x^2 + B_{2X} EI + \frac{P_{BX} EI}{T}\right) \left[-\frac{l_{BX}}{2}, \frac{l_{BX}}{2}\right] \\ -2\alpha_A^2 EI \{-A_{1X}[SS(x) - CS(x)] + A_{2X}[SC(x) - CC(x)]\} \left[\frac{l_{BX}}{2}, +\infty\right). \end{cases} \tag{13}$$

Similarly, the bending deformation equation of the thick hard roof in the stope space along the transverse direction of the working face (Y-axis) is as follows:

$$w_{ABY} = \begin{cases} A_{1Y} [CC(-y) - SC(-y)] + A_{2Y} [CS(-y) - SS(-y)] \left(-\infty, -\frac{l_{BY}}{2}\right) \\ \frac{P_{BY}}{24EI} y^4 + \frac{B_{2Y}}{2} y^2 + B_{4Y} \left[-\frac{l_{BY}}{2}, \frac{l_{BY}}{2}\right] \\ A_{1Y} [CC(y) - SC(y)] + A_{2Y} [CS(y) - SS(y)] \left[\frac{l_{BY}}{2}, +\infty\right), \end{cases} \tag{14}$$

$$M_{ABY} = \begin{cases} -2\alpha_A^2 EI \{-A_{1Y}[SS(-y) - CS(-y)] + A_{2Y}[SC(-y) - CC(-y)]\} \left(-\infty, -\frac{l_{BY}}{2}\right) \\ -\left(\frac{P_{BY}}{2} y^2 + B_{2Y} EI + \frac{P_{BY} EI}{T}\right) \left[-\frac{l_{BY}}{2}, \frac{l_{BY}}{2}\right] \\ -2\alpha_A^2 EI \{-A_{1Y}[SS(y) - CS(y)] + A_{2Y}[SC(y) - CC(y)]\} \left[\frac{l_{BY}}{2}, +\infty\right), \end{cases} \tag{15}$$

and

$$\begin{cases} B_{2Y} = \frac{P_{BY} l_{BY}}{8\alpha_A EI} \left(\frac{1}{-\frac{l_{BY}}{4\alpha_A} - \frac{1}{2\alpha_A^2}}\right) \left(\frac{1}{\alpha_A^2} + \frac{l_{BY}^2}{12} + \frac{l_{BY}}{2\alpha_A}\right) - \frac{P_{BY}}{T}, \\ B_{4Y} = \frac{P_{BY} l_{BY}}{8EI} \left(\frac{1}{\alpha_A^3} - \frac{l_{BY}^2}{16\alpha_A} - \frac{l_{BY}^3}{48} - \frac{2EI}{\alpha_A T}\right) - B_{2Y} \left(\frac{l_{BY}}{4\alpha_A} + \frac{l_{BY}^2}{8}\right), \\ A_{1Y} = \frac{P_{BY} l_{BY}}{8EI} \left(\frac{1}{\alpha_A^3} - \frac{l_{BY}^2}{16\alpha_A}\right) - \frac{l_{BY}}{4\alpha_A} \left(B_{2Y} + \frac{P_{BY}}{T}\right), \\ A_{2Y} = \frac{P_{BY} l_{BY}}{8EI} \left(\frac{1}{\alpha_A^3} + \frac{l_{BY}^2}{16\alpha_A}\right) + \frac{l_{BY}}{4\alpha_A} \left(B_{2Y} + \frac{P_{BY}}{T}\right), \end{cases} \tag{16}$$

Based on the Marcus simplified algorithm, the orthogonal slab structural units along the mining direction (X-axis) and the transverse direction (Y-axis) of the working face meet the following requirements:

$$w_{ABX}|_{x=0} = w_{ABY}|_{y=0} \tag{17}$$

Substituting **Formulas 11–16**, the result is as follows:

$$\frac{p_{BX}}{p_{BY}} = \frac{\left[\frac{l_{BY}}{8} \left(\frac{1}{\alpha_A^3} - \frac{l_{BY}^2}{16\alpha_A} - \frac{l_{BY}^3}{48} \right) - \frac{EI l_{BY}}{4\alpha_A T} + \frac{l_{BY}}{8\alpha_A} \left(\frac{1}{\alpha_A^2} + \frac{l_{BY}^2}{12} + \frac{l_{BY}}{2\alpha_A} \right) + \frac{EI}{T} \left(\frac{l_{BY}}{4\alpha_A} + \frac{1}{2\alpha_A^2} \right) \left(\frac{l_{BY}}{4\alpha_A} + \frac{l_{BY}^2}{8} \right) \right]}{\left[\frac{l_{BX}}{8} \left(\frac{1}{\alpha_A^3} - \frac{l_{BX}^2}{16\alpha_A} - \frac{l_{BX}^3}{48} \right) - \frac{EI l_{BX}}{4\alpha_A T} + \frac{l_{BX}}{8\alpha_A} \left(\frac{1}{\alpha_A^2} + \frac{l_{BX}^2}{12} + \frac{l_{BX}}{2\alpha_A} \right) + \frac{EI}{T} \left(\frac{l_{BX}}{4\alpha_A} + \frac{1}{2\alpha_A^2} \right) \left(\frac{l_{BX}}{4\alpha_A} + \frac{l_{BX}^2}{8} \right) \right]} \tag{18}$$

Based on the MARCUS simplified algorithm, given that $p_{BX} + p_{BY} = p_B$, let $\lambda_B = p_{BX}/p_{BY}$; then, the strip loads of the thick hard roof structure along the working face direction (X-axis) and the strip loads along the working face transverse direction (Y-axis) are respectively, as follows:

$$\begin{cases} p_{BX} = \frac{\lambda_B p_B}{1 + \lambda_B} \\ p_{BY} = \frac{p_B}{1 + \lambda_B} \end{cases} \tag{19}$$

According to the energy principle, the integral equation of the elastic energy accumulation density U of the strip structure of the thick hard roof is as follows:

$$dU = \int_0^\kappa M d\kappa, \tag{20}$$

where κ is the curvature of the strip member.

According to the physical equation of the linear elastic strip member, it can be seen that

$$M = EI\kappa, \tag{21}$$

According to the geometric equation of the strip member with a linear elastic medium, it can be seen that

$$\kappa = d\theta/dx, \tag{22}$$

Simultaneously, **Eqs 14–16** are sorted as follows:

$$dU = \frac{EIM^2}{2}, \tag{23}$$

According to the bending moment equation under the mining bearing of the thick hard roof of the mining overburden derived from **Eqs 3 and 8**, and substituting them into **Eq. 23**, the elastic energy accumulation density equation under the mining bearing state of the thick hard roof is as follows:

$$dU_{ABX} = \begin{cases} 2\alpha_A^4 EI \{ -A_{1X} [SS(-x) - CS(-x)] + A_{2X} [SC(-x) - CC(-x)] \}^2 & \left(-\infty, -\frac{l_{BX}}{2} \right) \\ \frac{EI}{2} \left(\frac{p_{BX}}{2EI} x^2 + B_{2X} + \frac{p_{BX}}{T} \right)^2 & \left[-\frac{l_{BX}}{2}, \frac{l_{BX}}{2} \right] \\ 2\alpha_A^4 EI \{ -A_{1X} [SS(x) - CS(x)] + A_{2X} [SC(x) - CC(x)] \}^2 & \left[\frac{l_{BX}}{2}, +\infty \right) \end{cases} \tag{24}$$

Mechanical Law of the Mining Bearing Capacity and Energy Accumulation of the Thick Hard Roof

Using the example analysis, the mechanical characteristics of the mining bearing capacity and energy accumulation evolution of the thick hard roof are revealed. The assumptions for example analysis are the following: $l_{BX} = 60$ m, $d = 10$ m, $b = 1$, $E = 4$ GPa, $\nu = 0.2$, $k = 1000$ MN/m, and $p_{BX} = 1$ MPa. The above parameters are, respectively, substituted into the deflection equation (**Eq. 12**), bending moment equation (**Eq. 13**), and elastic energy accumulation density (**Eq. 24**) to analyze the influencing factors of the mining bearing capacity of the thick hard roof. The calculation results are shown in **Figures 4–7**.

(1) Influence of the Overlying Load on the Mining Bearing Capacity of the Thick Hard Roof.

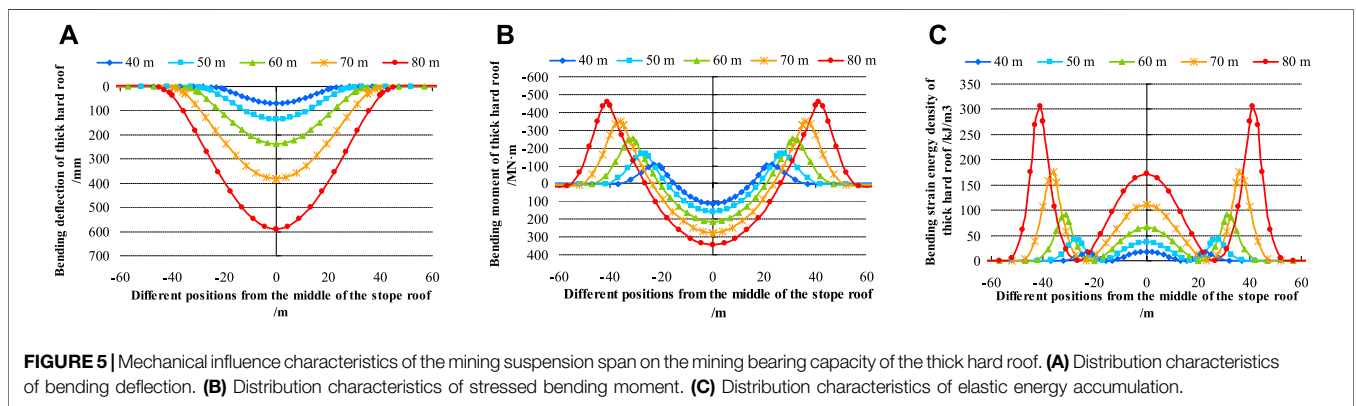
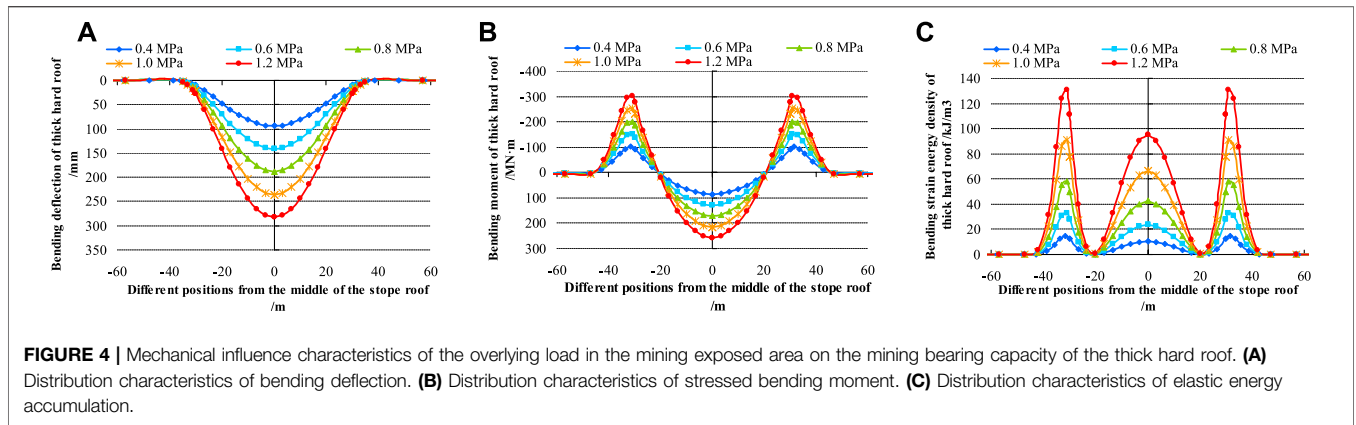
As shown in **Figure 4**, with the increase of the overburden transmission load, the mining bearing state and energy accumulation of the thick and hard roof are significantly intensified, leading to a more serious and hidden danger of mining instability of thick and hard roof; from the mechanical distribution characteristics of mining bearing, the bending force and accumulated energy of the thick and hard roof are mainly concentrated in the middle and both ends of the mining exposed area; among them, the position near the end of the suspended area (1–5 m away from the boundary of the suspended area) is the key position to judge the mining failure and instability of the thick and hard roof.

(2) Influence of the Mining Suspension Span on the Mining Bearing Capacity of the Thick Hard Roof.

As shown in **Figure 5**, with the increase of the overhang span, the bearing load of the thick and hard roof in the mining overhang area increases, and the bending degree and accumulated energy density of the thick and hard roof show an increasing evolution. The mining energy accumulation of the thick and hard roof is particularly sensitive to the increase of the overhang span.

(3) Influence of the Rock Stratum Thickness on the Mining Bearing Capacity of the Thick Hard Roof.

As shown in **Figure 6**, the greater the thickness of the rock stratum, the greater the bending stiffness of the rock stratum, making the thick and hard roof have a stronger bearing and energy accumulation capacity; although the bending degree of the



thick and hard roof decreases and the peak value of the bending moment does not change significantly, excessive energy accumulation will cause strong mining instability and dynamic pressure in the stope space, and the bending moment in the mining bearing area shows the characteristics of weakening convergence distribution.

(4) Influence of the Rock Elastic Modulus on the Mining Bearing Capacity of the Thick Hard Roof.

As shown in **Figure 7**, the influence of the elastic modulus of the rock stratum on the mechanical bearing capacity of the thick and hard roof is similar to the influence characteristics of the thickness of the rock stratum, and the bending stiffness of the rock stratum itself is improved, which leads to the increase of the mining breaking limit span. Accordingly, the mining instability energy and impact dynamic pressure are more intense when the mining instability occurs.

To sum up, the thick hard roof has the characteristics of a strong bearing capacity and large accumulation of mining energy, and the working face is strongly affected by the dynamic pressure; the greater the thickness and elastic modulus of the thick hard roof, the greater its flexural stiffness, and the ultimate breaking span of the thick hard roof increases; with the increase of the overhanging span and overlying load of the thick hard roof, its

mining bearing state and energy accumulation are evidently intensified.

INFLUENCE OF THE ACCUMULATED ENERGY RELEASE OF THICK HARD ROOF MINING ON THE DYNAMIC LOAD OF THE HYDRAULIC SUPPORT IN THE WORKING FACE

Elastic Energy Release of Mining Failure and Instability of the Thick Hard Roof

According to the distribution characteristics of the mining bearing capacity and energy accumulation evolution of the thick hard roof given in the *Mechanical Law of Mining Bearing Capacity and Energy Accumulation of the Thick Hard Roof* section, the tensile fracture of the upper boundary of the thick hard roof is selected as the judgment condition of mining fracture instability, and its bending expression is as follows:

$$\max|M_{ABX}(x)| \geq [\sigma_t]d^2/6, \tag{25}$$

where $[\sigma_t]$ is the tensile strength of the thick hard roof rock stratum.

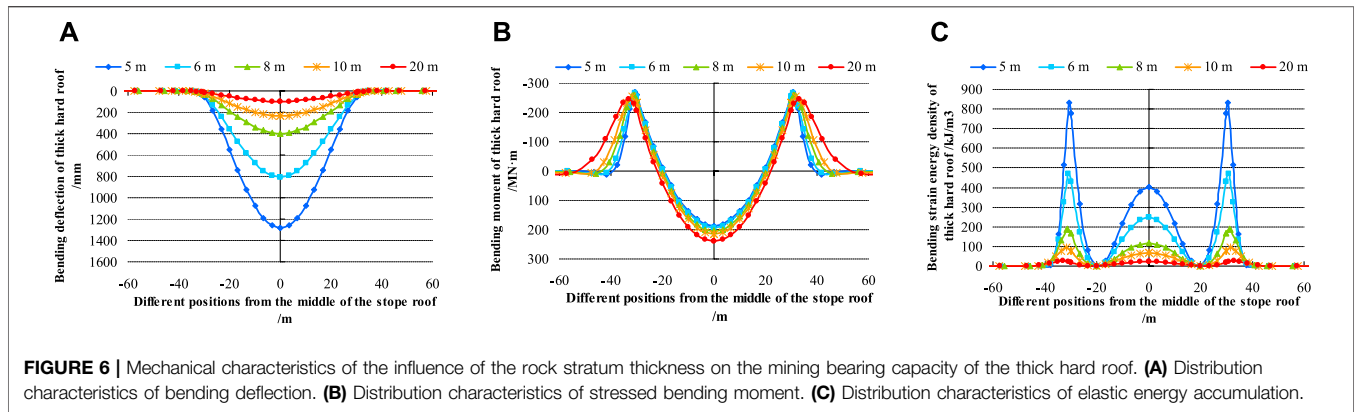


FIGURE 6 | Mechanical characteristics of the influence of the rock stratum thickness on the mining bearing capacity of the thick hard roof. **(A)** Distribution characteristics of bending deflection. **(B)** Distribution characteristics of stressed bending moment. **(C)** Distribution characteristics of elastic energy accumulation.

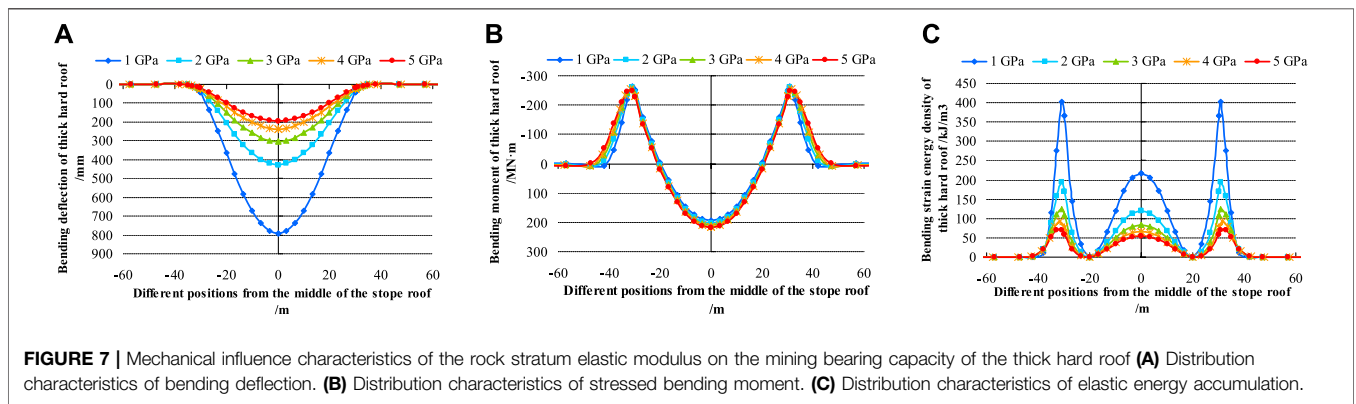


FIGURE 7 | Mechanical influence characteristics of the rock stratum elastic modulus on the mining bearing capacity of the thick hard roof **(A)** Distribution characteristics of bending deflection. **(B)** Distribution characteristics of stressed bending moment. **(C)** Distribution characteristics of elastic energy accumulation.

By substituting the bending moment equation (Eq. 13) of the thick hard roof into Eq. 24, the discrimination equation of mining failure and instability of the thick hard roof is obtained.

$$\max | -2k\alpha_A^2 EI \{ -A_{1X} [SS(x) - CS(x)] + A_{2X} [SC(x) - CC(x)] \} | \geq \frac{[\sigma_t] d^2}{6}, \quad (26)$$

The example analysis shows that the mining breaking span and mining suspension span are not in the same position, and the mining limit breaking span l_{AB} of the thick hard roof can be calculated by Eq. 26. At the moment of mining breaking and instability, the elastic energy accumulated by the mining bearing of the thick hard roof is released due to breaking and instability, which is transformed into the instability kinetic energy of the broken block, and the mining elastic energy of the thick hard roof within the range of $(-l_{ABX}/2, l_{ABX}/2)$ is integrated, the elastic energy release equation U_{wJBDX} of the thick hard roof breaking instability is obtained from the equation.

$$U_{wJBDX} = \int_{-l_{ABX}/2}^{l_{ABX}/2} dU_{ABX} dx, \quad (27)$$

By integrating the above formula, the elastic energy release equation U_{wJBDX} of mining failure and instability of the thick hard roof is obtained as follows:

$$U_{wJBDX} = \frac{P_{BX}^2 l_{BX}^3}{620EI} + \frac{P_{BX} l_{BX}^3}{2A} \left(B_{2X} + \frac{P_{BX}}{T} \right) + \frac{EI l_{BX}}{2} \left(B_{2X} + \frac{P_{BX}}{T} \right)^2 + 4\alpha_A^4 EI \left\{ \frac{e^{-2\alpha_A \left(\frac{l_{ABX}}{2} - \frac{l_{BX}}{2} \right)}}{8\alpha_A} \left[(2A_{1X} A_{2X} - A_{2X}^2 + A_{1X}^2) \cos 2\alpha_A \left(\frac{l_{ABX}}{2} - \frac{l_{BX}}{2} \right) + (2A_{1X} A_{2X} + A_{2X}^2 - A_{1X}^2) \sin 2\alpha_A \left(\frac{l_{ABX}}{2} - \frac{l_{BX}}{2} \right) \right] - \frac{(A_{2X}^2 + A_{1X}^2)}{4\alpha_A} \left[e^{-2\alpha_A \left(\frac{l_{ABX}}{2} - \frac{l_{BX}}{2} \right)} - 1 \right] - \frac{2A_{1X} A_{1X} - A_{2X}^2 + A_{1X}^2}{8\alpha_A} \right\} \quad (28)$$

Dynamic Load Response of the Hydraulic Support in the Working Face Under Thick Hard Roof Conditions

As shown in Figure 8, the mining instability of a thick hard roof leads to the release of elastic energy accumulated by the thick hard roof. At the same time, with the work done by the overlying load, they are jointly converted into the mining instability kinetic energy of the thick hard roof, forming a dynamic load impact on the directly broken roof below; the impact dynamic load is transmitted to the hydraulic support of the working face along the longitudinal direction to form the dynamic pressure of the working face.

According to this force transmission characteristic, the dynamic load response of the hydraulic support in the working face with an accumulated energy release of thick hard roof mining is analyzed, and the energy balance equation before

and after mining instability of the thick hard roof is established according to the energy conservation:

$$p_{BX}l_{ABX}\Delta w_{ABX} + U_{w_{ABX}} = V_{ABX}, \quad (29)$$

where V_{ABX} is the kinetic energy of mining failure and instability of the thick hard roof, $V_{ABX} = \int_0^{\Delta w_{ABX}} K_{ZJD} w dw = \frac{1}{2} K_{ZJD} \Delta w_{ABX}^2$; K_{ZJD} is the stiffness of the coal rock direct roof; Δw_{ZJDX} is the movement of the thick hard roof instability.

Solution:

$$\Delta w_{ABX} = \frac{p_{BX}l_{ABX} + \sqrt{(p_{BX}l_{ABX})^2 + 2K_{ZJD}U_{w_{BDX}}}}{K_{ZJD}}, \quad (30)$$

Eq. 29 is substituted into Eq. 28, and it is concluded that the impact dynamic load Q_{ZJD} caused by the mining instability of the thick hard roof on the direct roof is as follows:

$$Q_{ABX} = K_{ZJD}\Delta w_{ZJDX} = p_{BX}l_{ABX} \left[1 + \sqrt{1 + \frac{2K_{ZJD}U_{w_{BDX}}}{(p_{BX}l_{ABX})^2}} \right], \quad (31)$$

It should be noted that due to the mining fracture and block hinged rotation shown in Figure 2 when the thick hard roof is unstable, part of the accumulated energy released by the thick hard roof mining is transmitted to the goaf floor and the other part is transmitted to the coal and rock direct roof at the hinged points at both ends. Therefore, the effective impact dynamic load borne by the direct roof above the working face is $Q_{ZJD} = Q_{ABX}/4$.

As shown in Figure 9, the dynamic load response analysis of the hydraulic support in the working face is based on the hydraulic support in the middle of the working face. In the mining space of the working face, the mining impact dynamic load at each point of the thick hard roof will have a superimposed impact on the dynamic load transmission of the hydraulic support. In view of the influence of the mining space, this study analyzes the influence of dynamic load superposition of the middle support of the working face with the idea of semi-infinite body mechanical analysis under uniformly distributed load conditions.

Considering the top of the hydraulic support in the middle of the working face as the origin o, the horizontal direction along the working face is the Y-axis, and the vertical direction is the Z-axis. The impact dynamic load Q_{ZJD} can be calculated by Eq. 31; considering that the hydraulic support resistance of the longwall working face is composed of the gravity load of the direct roof of coal and rock and the effective impact dynamic load transmitted from the direct roof, in which the gravity load G_{ZJD} of the inclined rectangular block of the direct roof of coal and rock carried by the roof of the support is as follows:

$$G_{ZJD} = \gamma_{ZJD} g d_{ZJD} b_{ZJ} \frac{(2l_{ZJ} + d_{ZJD} \cot \beta)}{2}, \quad (32)$$

where l_{ZJ} is the top control distance of the hydraulic support of the working face; β_{ZJD} is the direct roof breaking angle of coal and rock; r_{ZJD} is the average unit weight of the direct roof of coal and rock; g is the acceleration of gravity; and b_{ZJ} is the center distance of the support.

To sum up, the dynamic load response estimation equation F_{ZJ} of the hydraulic support in the working face with the thick hard roof is established as follows:

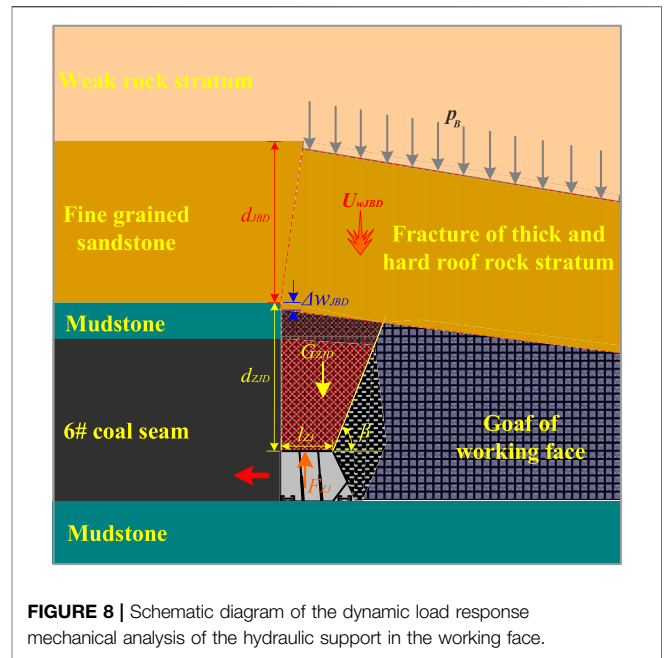


FIGURE 8 | Schematic diagram of the dynamic load response mechanical analysis of the hydraulic support in the working face.

$$\begin{aligned} F_{ZJ} &= G_{ZJD} + \int_{-\frac{L}{2}}^{\frac{L}{2}} s Q_{ZJD} b_{ZJ} [d_{ZJD}^2 + y^2]^{-\frac{\eta}{2}} dy \\ &= \gamma_{ZJD} g d_{ZJD} b_{ZJ} \frac{(2l_{ZJ} + d_{ZJD} \cot \beta)}{2} + 2s Q_{ZJD} b_{ZJ} \int_0^{\frac{L}{2}} [d_{ZJD}^2 + y^2]^{-\frac{\eta}{2}} dy, \end{aligned} \quad (33)$$

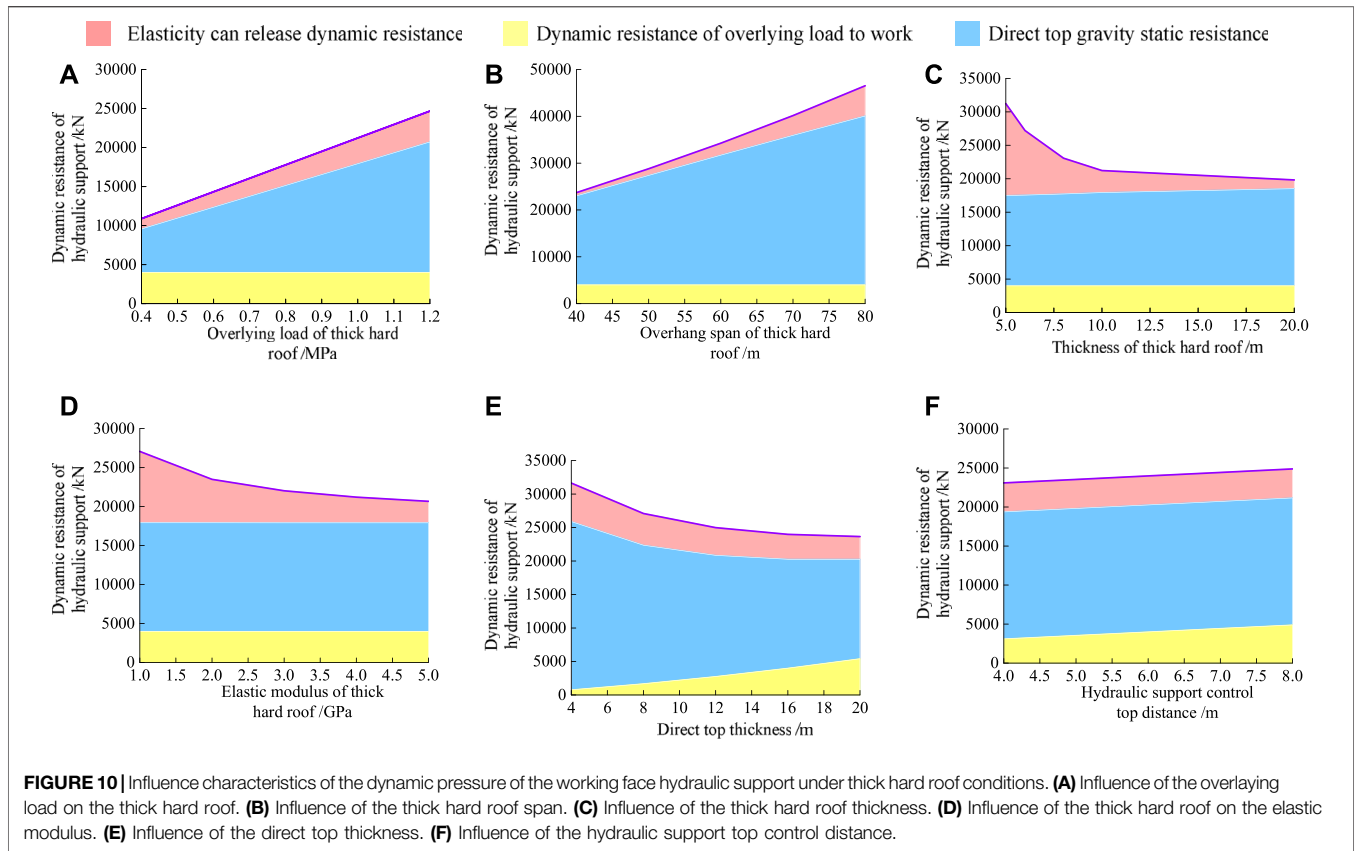
where L is the width of the working face; η is the attenuation coefficient of dynamic load transmission of the direct roof rock medium $\eta \geq 1$, and the greater the η , the greater the attenuation degree of the dynamic load (Gao et al., 2007; Jiang et al., 2015); and s is the dynamic load transfer efficiency. According to the analysis of the propagation efficiency and attenuation law of vibration energy in the literature (Gao et al., 2007; Jiang et al., 2015), the dynamic load transfer efficiency is generally 1/100–1/10.

Considering in this calculation $\eta = 1.0$ and $s = 1/20$, the dynamic load response estimation equation F_{ZJ} of the hydraulic support of the working face under the condition of a thick hard roof is obtained by integrating Eq. 34:

$$\begin{aligned} F_{ZJ} &= \gamma_{ZJD} g d_{ZJD} b_{ZJ} \frac{(2l_{ZJ} + d_{ZJD} \cot \beta)}{2} + \frac{Q_{ZJD} b_{ZJ}}{10} \left[\ln \left(\frac{L}{2} \right. \right. \\ &\quad \left. \left. + \sqrt{\frac{L^2}{4} + d_{ZJD}^2} \right) - \ln(d_{ZJD}) \right], \end{aligned} \quad (34)$$

Dynamic Load Response Characteristics of the Hydraulic Support in the Thick Hard Roof Working Face

Based on the example analysis given in the *Analysis of the Mining Bearing Mechanical Model of the Thick Hard Roof* section, the dynamic load response characteristics of the hydraulic support in



dynamic pressure. In view of the safety problems of underground coal mining engineering, this study suggests adopting pre-splitting and roof cutting technology to transform the basic mechanical bearing state of the thick hard roof, shorten the mining breaking span of the thick hard roof, and reduce the dynamic pressure appearance strength of the thick hard roof.

Technical Countermeasures for Roof Cutting and Pressure Relief of the Thick Hard Roof Working Face

Comprehensively considering the coal measures and geological conditions of a fully mechanized top-coal caving face and the actual situation of top-coal caving mining, the technical scheme of blasting top cutting in the initial mining stage of the fully mechanized top-coal caving face is designed, as shown in Figure 11.

The top cutting blasting drilling hole is arranged at the side of the roadway 500 mm behind the cutting hole of the working face, and within the range of the mining roadway 50 m away from the cutting hole mining coal wall and 500 mm near the side of the coal pillar with $\Phi 70 \text{ mm} \times 4000 \text{ mm}$ and drilling spacing of 800 mm. The two-way shaped charge blasting technology is adopted. The outer diameter of the long axis of the specially shaped charge tube is 49 mm, the outer diameter of the short axis is 41 mm, and the tube length is 1500 mm. The explosive is a grade II coal mine emulsion explosive with a

specification of $\Phi 35 \times 300 \text{ mm/roll}$; the blasting hole is sealed with blasting mud, and the blasting network connection is connected in series with a detonating cord.

Feedback on the Bearing Effect of the On-Site Hydraulic Support

The mining starts from the cutting hole of the working face, and the pressure bearing condition of the hydraulic support of the fully mechanized top-coal caving working face after the roof cutting on-site is monitored. The hydraulic support is selected in the middle of the working face (52#, 70#) and near the end of the working face (31#, 118#), as shown in Figure 11 to collect the ground pressure monitoring data. The data acquisition results of ground pressure monitoring are shown in Figure 12.

As shown in Figure 12, since the coal wall of the cut roadway began to be mined, the resistance of the working face 31# support increases at 27–30 m of mining, with the maximum working resistance of 37.6 MPa and the duration of the pressure of 16 h; the working face 52# support shows the phenomenon of increasing resistance at 27–29 m of mining, with the maximum working resistance of 37.3 MPa and the incoming pressure lasts for 4 h; the working face 70# support shows the phenomenon of increasing resistance at 26–28 m of mining, with the maximum working resistance of up to 38 MPa and the incoming pressure lasts for 2.5 h; the working face 118# support shows the phenomenon of increasing resistance at

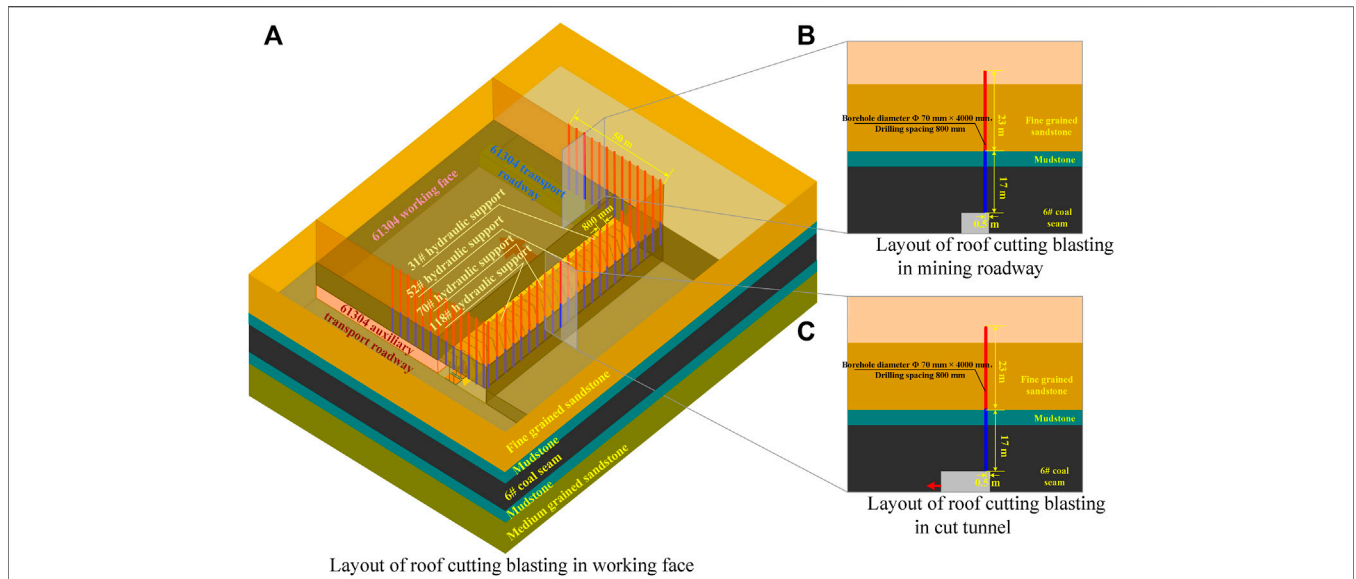


FIGURE 11 | Schematic diagram of blasting roof cutting technology at the working face (A) Layout of roof cutting blasting in the working face. (B) Layout of roof cutting blasting in the mining roadway. (C) Layout of roof cutting blasting in the cut tunnel.

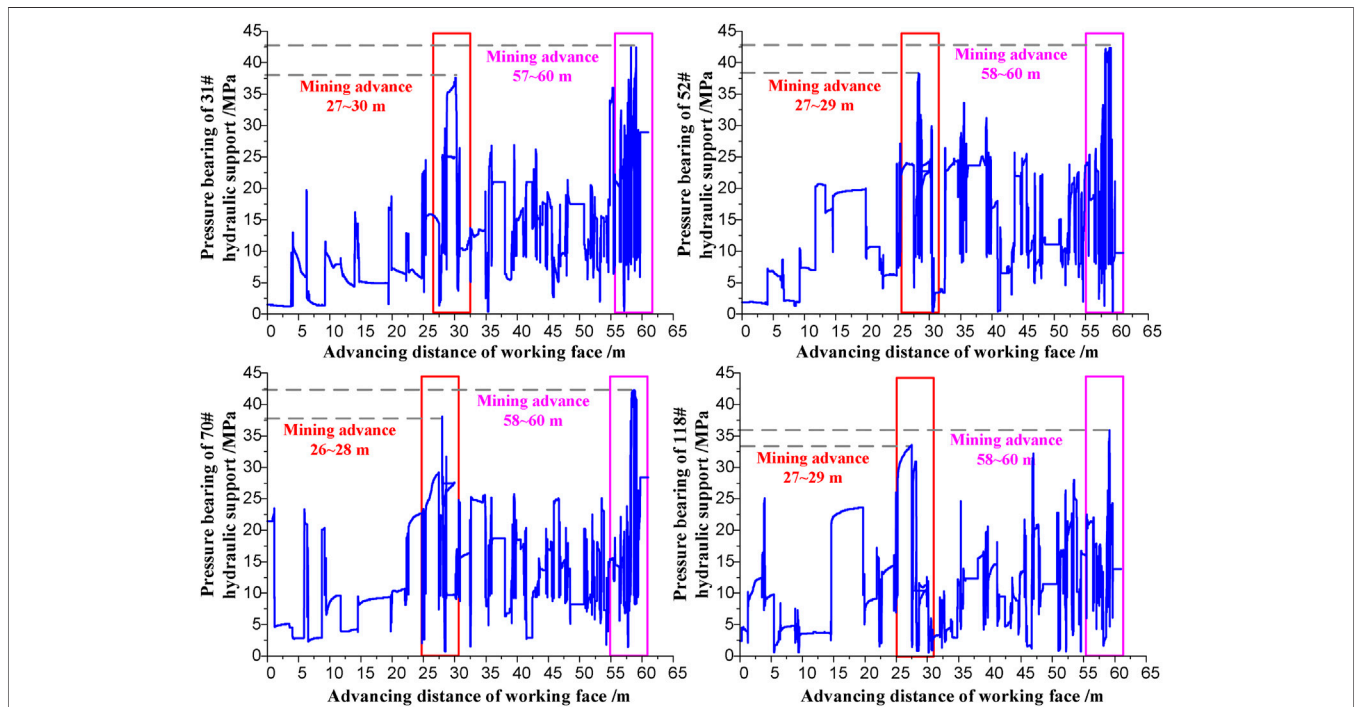


FIGURE 12 | Pressure monitoring of the working face hydraulic support (starting from the coal wall of the cut roadway).

27–29 m of mining, with the maximum working resistance of 33.6 MPa and the incoming pressure lasts for 21 h; after that, at a position of 57–60 m, the resistance of hydraulic supports increased again and the working resistance was 39–44 MPa.

The on-site monitoring results show that the ground pressure of the roof cut occurs when the mining is 26–30 m, that is, the thick hard

roof of the working face is broken and unstable, and the maximum dynamic incoming pressure of the hydraulic support of the working face is 38 MPa (i.e., dynamic resistance: 14500 kN) which is less than the working resistance of the hydraulic support of the working face (working resistance of the hydraulic support of the ZF18000/28/45 working face is 18000 kN), the hydraulic support of the on-site

working face has stable bearing and no equipment damage; by monitoring the subsequent mining stage, the dynamic incoming pressure of the hydraulic support of the working face is in the range of 43 MPa (i.e., dynamic resistance: 13800–16400 kN), the blasting roof cutting scheme of the fully mechanized top-coal caving face has achieved the expected ground pressure control effect and avoided the safety disaster of strong dynamic pressure caused by the mining instability of the thick hard roof.

CONCLUSION

- (1) The greater the thickness and elastic modulus of the thick hard roof, the greater the flexural stiffness and the ultimate breaking span of the thick hard roof increases; with the increase of the overhanging span and overlying load of the thick hard roof, its mining bearing state and energy accumulation are obviously intensified.
- (2) The dynamic resistance of the hydraulic support in the working face with a thick hard roof is composed of the dynamic resistance caused by the release of elastic energy accumulated by the mining of the thick hard roof and the work of the overlying load, as well as the static resistance caused by the direct roof gravity; among them, the dynamic resistance caused by the work of the overlying load accounts for the highest proportion, followed by the dynamic resistance caused by the release of elastic energy accumulated by the mining of the thick hard roof.
- (3) The cause of mining instability and strong dynamic pressure of the thick hard roof lies in the large-span mining suspension. The long-span mining suspension structure of the thick hard roof leads to a high overlying load and serious energy accumulation and dispersion evolution, and strong dynamic load impact at the moment of mining instability.
- (4) Controlling the breaking span of the thick hard roof by adopting pre-splitting and roof cutting technology reduces the impact dynamic load caused by mining instability of

the thick hard roof, and effectively, eliminates the potential safety hazard of over limit bearing of the hydraulic support.

DATA AVAILABILITY STATEMENT

The original contributions presented in the study are included in the article/Supplementary Material, further inquiries can be directed to the corresponding author.

AUTHOR CONTRIBUTIONS

QB and MT carried out the mechanical analysis, and MT and XZ carried out technical design; QB, MZ, and QZ analyzed the data results, and QB and MT wrote the manuscript.

FUNDING

This research was funded by the National Natural Science Foundation of China (52074008, 52074007, and 52104114), the Natural Science Foundation of Anhui Province (2008085ME142), the Anhui Collaborative University Innovation Project (GXXT-2020-056), and the Open Research Fund Project of Key Laboratory of Safety and High-Efficiency Coal Mining of Ministry of Education (JYBSYS2019208).

ACKNOWLEDGMENTS

The authors thank Tangjiahui coal mine and the Anhui University of Technology for providing mine geological data and data analysis resources needed to complete this work.

REFERENCES

- Christopher, M., and Michael, G. (2016). Evaluating the Risk of Coal Bursts in Underground Coal Mines. *Int. J. Mining Sci. Tech.* 42 (1), 42–47. doi:10.1016/j.ijmst.2015.11.009
- Dou, L., Yang, K., Liu, W., Chi, X., and Wen, Z. (2020). Mining-induced Stress-Fissure Field Evolution and the Disaster-Causing Mechanism in the High Gas Working Face of the Deep Hard Strata. *Geofluids* 2020 (3), 1–14. doi:10.1155/2020/8849666
- Gao, M. S., Dou, L. M., Zhang, N., Mu, Z. L., and Yang, B. S. (2007). Experimental Study on Earthquake Tremor for Transmitting Law of Rockburst in Geomaterials. *Chin. J. Rock Mech. Eng.* 26 (7), 1365–1371. doi:10.1016/S1872-2067(07)60020-5
- Gao, R., Huo, B., Xia, H., and Meng, X. (2020). Numerical Simulation on Fracturing Behaviour of Hard Roofs at Different Levels during Extra-thick Coal Seam Mining. *R. Soc. Open Sci.* 7 (1), 191383. doi:10.1098/rsos.191383
- Gu, S., Jiang, B., Pan, Y., and Liu, Z. (2018). Bending Moment Characteristics of Hard Roof before First Breaking of Roof Beam Considering Coal Seam Hardening. *Shock and Vibration* 2018 (2), 1–22. doi:10.1155/2018/7082951
- He, H., Dou, L., Fan, J., Du, T., and Sun, X. (2012). Deep-hole Directional Fracturing of Thick Hard Roof for Rockburst Prevention. *Tunnelling Underground Space Tech.* 32, 34–43. doi:10.1016/j.tust.2012.05.002
- Iannacchione, A. T., and Tadolini, S. C. (2016). Occurrence, Prediction, and Control of Coal Burst Events in the U.S. *Int. J. Mining Sci. Tech.* 26 (1), 39–46. doi:10.1016/j.ijmst.2015.11.008
- Jiang, J., Wang, P., Wu, Q., and Zhang, P. (2016). Evolutionary Characteristics of Fracture Laws of High-Position Hard Thick Strata with Elastic Foundation Boundary. *J. China Univ. Mining Tech.* 45 (03), 490–499. doi:10.13247/j.cnki.jcumt.000512
- Jiang, J., Zhang, P., Qin, G., Li, F., Xu, B., and Xu, L. (2015). Breaking Law and Micro Seismic Energy Distribution of the High-Level Hard and Thick Key Layer on One Side Goaf. *J. Mining Saf. Eng.* 32 (4), 523–529. doi:10.13545/j.cnki.jmse.2015.04.001
- Ke, G. (2000). Bending Theories for Beams and Plates with Single Generalized Displacement. *Appl. Math. Mech.* 21 (09), 1091–1098. doi:10.1007/BF02459320

- Li, X., Ma, N., Zhong, Y., and Gao, Q. (2007). Storage and Release Regular of Elastic Energy Distribution in Tight Roof Fracturing. *Chin. J. Rock Mech. Eng.* 26 (S1), 2786–2793. doi:10.3321/j.issn:1000-6915.2007.z1.030
- Lu, C.-P., Liu, G.-J., Liu, Y., Zhang, N., Xue, J.-H., and Zhang, L. (2015). Microseismic Multi-Parameter Characteristics of Rockburst hazard Induced by Hard Roof Fall and High Stress Concentration. *Int. J. Rock Mech. Mining Sci.* 76, 18–32. doi:10.1016/j.ijrmms.2015.02.005
- Song, G., Wang, Z., and Zhong, X. (2020). Dynamic Impact Mechanism of Hard Roof Strata and Coupling Mechanism of "Constrain-Convergence" between Support and Surrounding Rock. *J. Mining Saf. Eng.* 37 (05), 951–959. doi:10.13545/j.cnki.jmse.2020.05.011
- Tan, Y., Zhang, M., Xu, Q., and Shitan, G. U. (2019). Study on Occurrence Mechanism and Monitoring and Early Warning of Rock Burst Caused by Hard Roof. *Coal Sci. Tech.* 47 (01), 166–172. doi:10.13199/j.cnki.cst.2019.01.023
- Xia, B., Jia, J., Yu, B., Zhang, X., and Li, X. (2017). Coupling Effects of Coal Pillars of Thick Coal Seams in Large-Space Stopes and Hard Stratum on Mine Pressure. *Int. J. Mining Sci. Tech.* 27 (06), 965–972. doi:10.1016/j.ijmst.2017.06.020
- Xie, S. R., Chen, D. D., Sun, Y. D., Gao, M. M., and Shi, W. (2016). Analysis on Thin Plate Model of Basic Roof at Elastic Foundation Boundary (I): First Breaking. *J. China Coal Soc.* 41 (06), 1360–1368. doi:10.13225/j.cnki.jccs.2016.0197
- Yang, S. L., Wang, J. C., and Yang, J. H. (2017). Physical Analog Simulation Analysis and its Mechanical Explanation on Dynamic Load Impact. *J. China Coal Soc.* 42 (2), 335–343. doi:10.13225/j.cnki.jccs.2016.6004
- Yang, S., Wang, J., and Li, L. (2020). Deformation and Fracture Characteristics of Key Strata Based on the Medium Thick Plate Theory. *J. China Coal Soc.* 45 (8), 2718–2727. doi:10.13225/j.cnki.jccs.2020.0366
- Yu, B., Liu, C. Y., Yang, J. X., and Liu, J. R. (2013). Research on the Fracture Instability and its Control Technique of Hard and Thick Roof. *J. China Univ. Mining Tech.* 42 (3), 342–348. doi:10.13247/j.cnki.jcmt.2013.03.003
- Zhang, J., Li, B., Zhou, N., and Zhang, Q. (2016). Application of Solid Backfilling to Reduce Hard-Roof Caving and Longwall Coal Face Burst Potential. *Int. J. Rock Mech. Mining Sci.* 88, 197–205. doi:10.1016/j.ijrmms.2016.07.025
- Zhang, M., Jiang, F., Chen, G., Jiao, Z., Hu, H., and Chen, B. (2020). A Stope Stress Transfer Model Based on the Motion State of Thick and Hard Rock Strata and its Application. *Chin. J. Rock Mech. Eng.* 39 (07), 1396–1407. doi:10.13722/j.cnki.jrme.2019.1118
- Zhang, M., Jiang, F., Keqing, L., Sun, C., and Zhai, M. (2017). A Study of Surface Seismic Damage Boundary Based on the Break and Movement of Extremely Thick Key Stratum. *J. China Univ. Mining Tech.* 46 (3), 514–520. doi:10.13247/j.cnki.jcmt.000672
- Zhao, T., Liu, C., Yetilmezsoy, K., Zhang, B., and Zhang, S. (2017). Fractural Structure of Thick Hard Roof Stratum Using Long Beam Theory and Numerical Modeling. *Environ. Earth Sci.* 76 (21), 1–7. doi:10.1007/s12665-017-7103-x
- Zuo, J. P., Sun, Y. J., and Qian, M. G. (2017). Movement Mechanism and Analogous Hyperbola Model of Overlying Strata with Thick Alluvium. *J. China Coal Soc.* 42 (06), 1372–1379. doi:10.13225/j.cnki.jccs.2016.1164

Conflict of Interest: The authors declare that the research was conducted in the absence of any commercial or financial relationships that could be construed as a potential conflict of interest.

Publisher's Note: All claims expressed in this article are solely those of the authors and do not necessarily represent those of their affiliated organizations, or those of the publisher, the editors, and the reviewers. Any product that may be evaluated in this article, or claim that may be made by its manufacturer, is not guaranteed or endorsed by the publisher.

Copyright © 2022 Bu, Tu, Zhang, Zhang and Zhao. This is an open-access article distributed under the terms of the Creative Commons Attribution License (CC BY). The use, distribution or reproduction in other forums is permitted, provided the original author(s) and the copyright owner(s) are credited and that the original publication in this journal is cited, in accordance with accepted academic practice. No use, distribution or reproduction is permitted which does not comply with these terms.